IEEE Access
Multidisciplinary ⋮ Rapid Review ⋮ Open Access Journal

Received 7 June 2023, accepted 7 July 2023, date of publication 24 July 2023, date of current version 27 July 2023.

Digital Object Identifier 10.1109/ACCESS.2023.3296254

RESEARCH ARTICLE

Stochastic Economic Operation of Coupling Unit of Flexi-Renewable Virtual Power Plant and Electric Spring in the Smart Distribution Network

MINGGUANG YAO[1,2], ZOHRE MORADI[3,4], SASAN PIROUZI[5], MOUSA MARZBAND[6], (Senior Member, IEEE), AND ALIASGHAR BAZIAR[3]

[1]School of Economics, Shanghai University, Shanghai 200444, China
[2]School of Tourism Leisure Management, Shanghai Institute of Tourism, Shanghai 201418, China
[3]Faculty of Engineering and Technology, Department of Electrical Engineering, Imam Khomeini International University, Qazvin 34149-16818, Iran
[4]Department of Biomaterials, Saveetha Dental College and Hospital, Saveetha Institute of Medical and Technical Sciences, Chennai 600077, India
[5]Department of Engineering, Semirom Branch, Islamic Azad University, Semirom 14778-93855, Iran
[6]Net Zero Industry Innovation Centre, Campus Masterplan, Teesside University, TS1 3BA Middlesbrough, U.K.

Corresponding authors: Mousa Marzband (M.Marzband@tees.ac.uk) and Mingguang Yao (yaomingguang2023@163.com)

This work was supported by the Decarbonising Transport through Electrification (DTE) Network+, a project funded by Engineering and Physical Sciences Research Council (EPSRC) under Grant EP/S032053/1.

ABSTRACT This paper outlines the operation of a Smart Distribution Network (SDN) that couples a Virtual Power Plant and Electric Springs (CVEs). In fact, CVEs participate simultaneously in energy and reactive service markets. The prime aim of the proposed scheme is to maximize the predicted profits of CVEs in the mentioned markets. The constraints in the problem formulation are the AC optimal power flow equations, flexibility limits in the network, and the operating model of CVEs. Further, the design is in a nonlinear formulation, which is followed by a linear approximation model to access a unique optimal response. Stochastic optimization is used to account for uncertainties in energy price, load, renewable power, and energy consumption of mobile storage devices. In addition, the results from implementing the design on the IEEE 69-bus SDN confirm the potential of CVEs to enhance the network's operation and access significant profits for power sources, storage devices, and responsive load. Finally, the design achieved 100% flexibility for the SDN through proper management of CVEs, resulting in an improvement of operating indices between 15-97% compared to power flow studies. Moreover, the CVEs profit in the modeling of uncertainties reduces approximately 19.6% compared to the deterministic model of the proposed scheme under complete flexibility conditions.

INDEX TERMS Electric spring, energy market, flexibility limit, reactive market, smart distribution network, virtual power plant.

NOMENCLATURE

INDICES

- b Bus.
- i CVE .
- j Line segment in the piecewise linearization technique.
- k Bus.
- w Scenario.
- τ Operation hour.
- ω Sides of a regular polygon.

DECISION VARIABLES

- F Profit of CVEs in energy and reactive power markets ($).
- P_{CH}, P_{DCH} Active power of charge and discharge (p.u.).
- P_{CVE}, Q^{+}_{CVE} Active and reactive power of CVE (p.u.).
- P^{+}_{CVE}, P^{-}_{CVE} Positive and negative components of PCVE (p.u.).

The associate editor coordinating the review of this manuscript and approving it for publication was Roberto C. Ambrosio.

P_{DR}, P_{VPP}	Active power of DRP and virtual power plant (VPP) (p.u.).
P_{DL}, Q_{DL}	Active and reactive power of the distribution line (p.u.).
P_{DS}, Q_{DS}	Active and reactive power of the distribution substation (p.u.).
P_{LO}	Active power loss of ES (p.u.).
V, ΔV	Voltage amplitude and voltage deviation (p.u.).
σ	Voltage angle (rad).

PARAMETERS

A	Incidence matrix of buses and CVEs (the element i,b is 1 if the ith CVE is connected to bus b; otherwise, it is 0.).
B	Incidence matrix of buses and distribution lines (the element b,k is 1 if the distribution line is between buses b and k; otherwise, it is 0.).
b_{DL}, g_{DL}	Susceptance and conductance of the distribution line (p.u.).
C	Space vector of CVE in the network (element b of the vector is 1 if CVE is connected to bus b; otherwise is 0.).
CR, DR	Charge and discharge rate in the storage (p.u.).
E^{lo}, E^{in}, E^{up}	Minimum stored energy, initial energy, and maximum stored energy in the storage (p.u.).
K_Q	The ratio of reactive power price to energy price.
P_L, Q_L	Active and reactive load (p.u.).
P_{PV}, P_{WT}	Active power of photovoltaic (PV) and wind turbine (WT) (p.u.).
$S_{DL^{up}}$, $S_{DS^{up}}$, $S_{DL^{CVE}}$	Maximum apparent power of distribution line, distribution substation, and CVE (p.u.).
sl	Line slope in the piecewise linearization technique.
V^{LF}	Voltage amplitude in power flow studies (p.u.).
V^{lo}, V^{up}	Minimum and maximum amplitude of voltage (p.u.).
Z, I, P	Constant parameters in constant impedance, current, and power load model (ZIP).
α, β	Loss coefficients of electric spring (ES) in p.u.
α_F	Flexibility tolerance (p.u.).
η^{CH}, η^{DCH}	Charge and discharge efficiency of the storage.
ρ_E	Energy price ($/MWh).
ψ	Rate of participation of consumers in the demand response program (DRP).
$\Delta\sigma$	Angle deviation (rad).

I. INTRODUCTION

A. MOTIVATION

Nowadays, the use of renewable energy sources such as wind and solar systems is increasing globally, particularly in distribution networks, due to the clean electricity they produce with low pollution levels [1]. However, the high penetration of these resources with the advantages of producing clean energy at cheaper operating costs in the distribution network can negatively impact the system's operation and flexibility indices. Operation indices are voltage profile, energy waste, and distribution line congestion. If the integration of RESs in the network increases, overvoltage, network losses, and congestion of distribution lines will also increase [1]. A widely accepted understanding of flexibility involves adjusting the amount of energy generated and reconfiguring the system in response to market-determined prices [2]. Therefore, decreased flexibility in a network causes a mismatch between actual energy utilization during real-time operations and predicted energy use in day-ahead operation; hence, this discrepancy can lead to a fine or penalty for imbalance in the energy market [2]. This occurs because renewable energy sources (RESs) often have limited control and management, and consumers typically consume low-cost energy while network management prioritizes resources with low pollution levels. Therefore, these sources inject their energy generation capacity into the network, which is proportional to the weather conditions and their intermittent nature [1]. In particular, controllable resources are required with RESs to tackle this issue. Further, batteries and demand response programs (DRP) are generally suitable alternatives due to very low time constants [3].They are used to balance out fluctuations in renewable energy source power during real-time operation in comparison to day-ahead predictions In addition presence of these resources can also improve network operation indices and, that achieving such goals requires the proper energy management in distribution systems. The first step in desirable energy management in distribution systems is adopting a suitable aggregator, e.g. a virtual power plant (VPP) for generation units, storage equipment, and responsive loads [4]. Most importantly, through coordination between the aforementioned components and the operator, a Virtual Power Plant (VPP) can achieve an efficient schedule for both renewable and flexible energy sources. Further, coordination of the VPP operator and the distribution system operator (DSO) can optimize the operation of distribution systems by ensuring optimal scheduling for Virtual Power Plants (VPPs). Moreover, the electric springs (ESs) contains a bidirectional DC-AC converter which could control their load on the AC side [5], regulate voltage, and control active and reactive power simultaneously. Hence, the coupling of VPP and ES (CVE) can play a key role in the simultaneous

management of the mentioned parameters. This results in improved technical and economic performance indicators for the system. Additionally, the system can participate in various energy and auxiliary service markets, leading to benefits for Virtual Power Plants (VPPs).

B. LITERTURE REVIEW

Several research have been conducted on the operation of generation sources, storage, and responsive loads for the SDN. For example, in [6] and [7], the robust operation of the SDN with aggregation of electric vehicles (EVs) and distributed generations (DGs) has investigated. These components participate in both energy and reactive power markets, allowing for financial gain from these markets. According to research, the cost of charging electric vehicles (EVs) decreases by 30% when participating in both energy and reactive power markets, compared to not participating in these market. Moreover, the power management of EVs and DGs in the SDN has led to the reduction of energy losses in the 24-hour horizon while increasing the voltage profile. In [8], energy management (active power exchange) of generation units, storage equipment, and responsive loads in the form of microgrid (MG) tied to the distribution network is presented. In this reference, only the participation of MGs in the energy market is considered. Two-layer energy management has adopted, hence, MGs are divided into two main and subcategories. In the first layer, the operation of the mentioned elements under the management of the MG operator is considered. In the second layer, the operation of sub-MGs under the management of main MGs has studied. This resulted in low computational time, and more financial benefits for MGs compared to the independent management. A multi-objective optimization for the operation of MGs connected to the SDN in the presence of power sources and storage devices, is presented in [9]. Multi-objective optimization has been applied to simultaneously model the operation, reliability, and environmental indicators. This is also the case for the unbalanced distribution network in [10]. The studies in references [9] and [10] reveal that through optimal management of internal resources and storage, the MG operator can enhance various technical indices in the network, outperforming power flow studies, while also promoting clean energy. In [11] and [12], flexible operation of electric spring (ES)-coupled batteries in MG with renewable sources is modeled. The results confirm that the battery-ES coupling system can simultaneously control active and reactive power, therefore, they play a highly impact role in enhancing operation and flexibility indices as compared to power flow studies in MG's.

In addition, significant research have carried out in the field of VPP operation. Reference [13] presents a two-layer formulation for the presence of VPPs in the SDN. In the study, the upper level formulate the model with renewable resources and aggregation of EVs in the form of VPP in the energy and reserve markets. The operation of the SDN is mentioned at the lower-level problem to reduce energy losses and voltage deviations. Thereafter, Bender's decomposition method is used to solve the problem. In [14] and [15], a virtual power plant (VPP) format is studied to manage the integration of responsive loads and wind turbines in energy markets. The model focuses on the VPP's involvement in the DA and RT energy markets and the balance market. In addition, the generation power of wind turbines is associated with uncertainty, hence the bidding in these markets may differ. The balance market is used to compensate this issue. According to the results, the use of the VPP format for wind turbines compared to single VPP management can provide high flexibility and lower cost in the balance market. A similar study has been conducted in [16], with the difference of the VPP format, which has employed to coordinate the storage, wind turbine, and responsive loads.

In study [17], it is assumed that VPP elements can simultaneously control active and reactive power, while contributing to harmonic compensation of nonlinear loads. Accordingly, VPP have a great potential in enhancing operation indices and power quality. Further, the planning-operation model of VPPs in the SDN has been studied in [18]. In this work, the siting and sizing of generation units and storage in the form of VPP significantly enhances the operating indices of the distribution system, with a minimal planning costs. References [19] and [20] examined the involvement of flexible VPPs consisting of PVs, hydro sources, and pumped storage in the energy market. Consequently, a two-step problem is analyzed. In the first step, the role of VPPs in the energy market is studied. Then, in the second step, a power correction model that takes into account the constraints imposed on irradiance, water, and environmental conditions for VPPs is analyzed. The bi-level operation of the active distribution network with VPPs was discussed in [21]. In the upper-level problem, the operation of the active distribution system is considered to minimize the operating costs, while the VPP operation to maximize its profit to provide ancillary services is considered in the lower-level problem. An optimal VPP energy management method is proposed in [22] for optimal energy and operating reserve scheduling. VPP operator has to make decisions based on the uncertainty coming from the stochastic variable renewable energy, load demand, as well as market electricity price. Thus, a dynamic risk reserve quantification method is proposed to cover both variable renewable power and load forecast uncertainties, while information gap decision theory is applied in the unit commitment procedures to study the impact of price uncertainty on the decision-making of VPP operators. References [23] and [24] proposes a statistical measure and a stochastic optimization model for generating risk-seeking wind power offering strategies in electricity markets. Inspired by the value at risk (VaR) to quantify risks in the worst-case scenarios of a profit distribution, a statistical measure is proposed to quantify potential high profits in the best-case scenarios of a profit distribution, which is referred to as value at best (VaB) in the best-case scenarios. Then, a stochastic optimization model based on VaB is developed

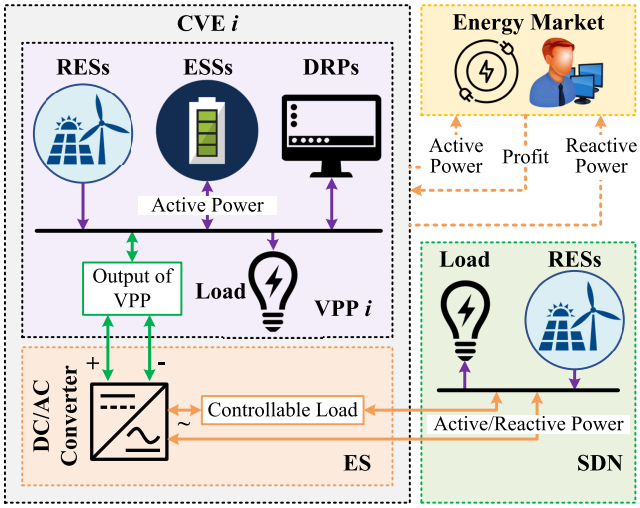

FIGURE 1. A framework of the suggested design.

for a risk-seeking wind power producer, which is formulated as a mixed-integer linear programming problem. In addition, Table 1 reports the abovementioned references in summary.

C. RESEARCH GAPS

According to Table 1, following gaps could be identified in operation of VPPs in SDNs:

noitemsep,nolistsep

- In most studies, the energy exchange model (active power) has been established in VPP and its components. However, several studies have a simultaneous exchange of active and reactive power of the VPP with the network and its internal elements. Under these conditions, a reactive power control element such as a DC-AC converter is used for each power source and storage. However, in the case of a CVE, its internal elements can only exchange energy with each other, which reduces the cost of the reactive power control element. Nonetheless, the ES, which is a DC-AC converter and has a controllable load on its AC side, which can control the reactive power flow with the network. Additionally, through adjusting the load on its AC side, the ES (Energy Storage) can regulate the voltage at the connection point with the grid, resulting in a nearly steady voltage profile across the network. However, that the ES and VPP coupling has rarely been addressed.
- VPP can be operated in energy and ancillary service markets simultaneously due to having various controllable elements such as non-renewable sources, storage, and responsive loads. In this regards, a suitable financial benefit is obtained for its elements. The topic of VPP participation in the energy market has received more attention in research, while the VPP model for participating in the reactive power or reactive ancillary services market has received comparatively less attention. Simultaneous, the examination of VPPs participating in both energy and auxiliary services markets has also received limited attention in research.
- Due to low operating cost and emission level, renewables have widespread applications in the power system. However, renewable energy sources produce unpredictable and inconsistent power output, as they rely on natural phenomena, thereby decreasing their flexibility. Different research adopts flexibility resources such as storage and responsive loads in the power system. Nonetheless, less research such as [11] and [25] state a numerical index for evaluation of system flexibility. Analysis of the status of an index requires its numerical value.

D. CONTRIBUTIONS

In order to address the identified research gaps and to provide coverage for these instances, this paper introduces the concept of stochastic operation of CVEs within the context of SDN, as depicted in Fig 1. In this figure, CVEs simultaneously participate in energy and reactive ancillary services (reactive power) markets. In the formulation, this plan is responsible for maximizing the expected profits of CVEs in the energy and reactive power markets. The constraints include the model of AC optimal power flow and flexibility limit in SDN in the presence of RESs; operating model of generation units, storage, and responsive loads in a VPP format; and ES formulation. Further, The proposed scheme features a nonlinear formulation, leading to varying solutions from different solvers, where the convergence time is also high. Therefore, the coefficient of confidence in its response is low [6], [8], [9], [10], [11]. However, in this study, a novel approach is presented, the Linear Approximation Model (LAM), which enables solvers to quickly determine a singular optimal solution In other words, in the distribution network, the voltage angle deviation of the two sending and receiving buses of a distribution line is generally smaller than 6 degrees [11], [13], [26]. By considering such an assumption as well as voltage magnitude linearization according to traditional piecewise linear linearization method, a suitable linear approximation model can be obtained for AC power flow in SDN, which has a low computational error [13]. In addition, the allowable capacity of distribution lines, substations, and ES generally has a circular plane. By substituting a regular polygon plane instead of a circular one, a linear approximation model with a small computational error is obtained for the permissible capacity of distribution lines, substations, and ES [13], [27]. Consequently, the design of the suggested approach incorporates a Linear Approximation Model with minimal computational error. Moreover, the parameters of load, market price, renewable power, and energy consumption of mobile storage devices (EVs) are uncertain. This method uses stochastic optimization to model them. Finally, the novelties of the present study could be listed as below:

noitemsep,nolistsep

- Modeling the simultaneous participation of CVEs in energy and reactive power market;

TABLE 1. A brief description of the literature.

Ref.	Coupling of VPP and ES	VPP participation in markets	Network flexibility limit model
[6]	✖	Energy and reactive power markets for distribution network	✖
[8]	✖	Energy market for micro-grids	✖
[9]	✖	✖	✖
[10]	✖	✖	✖
[11]	Coupling of battery and ES	✖	✓
[13]	✖	Energy market for VPP	✖
[14, 28]	✖	Energy market for VPP	✖
[16]	✖	Energy market for VPP	✖
[17]	✖	Energy market for VPP	✖
[18]	✖	✖	✖
[19]	✖	✖	✖
[21]	✖	✖	✖
[22, 29]	✖	Energy market for VPP	✖
[23]	✖	✖	✖
Current Scheme	✓	Energy and reactive power markets	✓

- Presenting the optimal operation of CVE in the SDN by considering the simultaneous management of active and reactive power and voltage regulation in the network;
- Mathematical modeling of flexibility index to investigate the network flexibility with CVEs.

E. PAPER ORGANIZATION

The layout of the paper includes 5 sections as described here. Section II states the formulation of the suggested scheme in both nonlinear and linear models. Section III describes the stochastic modeling of uncertainties. Numerical results are analyzed in Section IV. Eventually, Section V presents the conclusions.

II. SDN OPERATION WITH CVES

A. ORIGINAL NON-LINEAR FORMULATION

The deterministic formulation of SDN operation in the presence of CVEs is presented here. The plan is to maximize the predicted profits of CEVs in energy and reactive power markets, while at the same time adhering to the AC-OPF power flow limits and flexibility limit in the SDN and operation model of CVEs. Therefore, this plan is formulated as follows:

$$\max \quad F = \sum_{i,\tau,w} \pi_w \rho_{E\ \tau,w} \left(P_{CVE\ i,\tau,w} + K_Q Q_{CVE\ i,\tau,w}\right) \tag{1}$$

where

$$P_{DS\ b,\tau,w} + P_{PV\ b,\tau,w} + P_{WT\ b,\tau,w} + \sum_i A_{i,b} P_{CVE\ i,\tau,w} - \sum_k B_{b,k} P_{DL\ b,k,\tau,w} = (1 - C_b) P_{L\ b,\tau,w} + C_b P_{L\ b,\tau,w} \left(Z \left(\frac{V_{b,\tau,w}}{V^{LF}_{b,\tau,w}} \right)^2 + I \left(\frac{V_{b,\tau,w}}{V^{LF}_{b,\tau,w}} \right) + P \right) \quad \forall b, \tau, w \tag{2}$$

$$Q_{DS\ b,\tau,w} + \sum_i A_{i,b} Q_{CVE\ i,\tau,w} - \sum_k B_{b,k} Q_{DL\ b,k,\tau,w} = (1 - C_b) Q_{L\ b,\tau,w} + C_b Q_{L\ b,\tau,w} \left(Z \left(\frac{V_{b,\tau,w}}{V^{LF}_{b,\tau,w}} \right)^2 + I \left(\frac{V_{b,\tau,w}}{V^{LF}_{b,\tau,w}} \right) + P \right) \quad \forall b, \tau, w \tag{3}$$

$$P_{DL\ b,k,\tau,w} = g_{DL\ b,k} \left(V_{b,\tau,w}\right)^2 - V_{b,\tau,w} V_{k,\tau,w} \left\{ \begin{matrix} g_{DL\ b,k} \cos\left(\sigma_{b,\tau,w} - \sigma_{k,\tau,w}\right) + \\ b_{DL\ b,k} \sin\left(\sigma_{b,\tau,w} - \sigma_{k,\tau,w}\right) \end{matrix} \right\} \quad \forall b, k, \tau, w \tag{4}$$

$$Q_{DL\ b,k,\tau,w} = -g_{DL\ b,k} \left(V_{b,\tau,w}\right)^2 + V_{b,\tau,w} V_{k,\tau,w} \left\{ \begin{matrix} b_{DL\ b,k} \cos\left(\sigma_{b,\tau,w} - \sigma_{k,\tau,w}\right) - \\ g_{DL\ b,k} \sin\left(\sigma_{b,\tau,w} - \sigma_{k,\tau,w}\right) \end{matrix} \right\} \quad \forall b, k, \tau, w \tag{5}$$

$$\sigma_{b,\tau,w} = 0 \quad \forall\ b = \text{Slack bus}, \tau, w \tag{6}$$

$$\sqrt{\left(P_{DL\ b,k,\tau,w}\right)^2 + \left(Q_{DL\ b,k,\tau,w}\right)^2} \le S^{up}_{DL\ b,k} \quad \forall b, k, \tau, w \tag{7}$$

$$\sqrt{\left(P_{DS\ b,\tau,w}\right)^2 + \left(Q_{DS\ b,\tau,w}\right)^2} \le S^{up}_{DS\ b} \quad \forall b = \text{Slack bus}, \tau, w \tag{8}$$

$$V^{lo}_b \le V_{b,\tau,w} \le V^{up}_b \quad \forall b, \tau, w \tag{9}$$

$$-\alpha_F \le P_{DS\ b,\tau,w} - P_{DS\ b,\tau,w=1} \le \alpha_F \quad \forall b = \text{Slack bus}, \tau, w \tag{10}$$

$$P_{VPP\ i,\tau,w} = P_{PV\ i,\tau,w} + P_{WT\ i,\tau,w} + P_{DR\ i,\tau,w} + \left(P_{DCH\ i,\tau,w} - P_{CH\ i,\tau,w}\right) - P_{L\ i,\tau,w} \forall i, \tau.w \tag{11}$$

$$-\psi_i P_{L\ i,\tau,w} \le P_{DR\ i,\tau,w} \le \psi_i P_{L\ i,\tau,w} \quad \forall i, \tau, w \tag{12}$$

$$\sum_{\tau} P_{DR\ i,\tau,w} = 0 \quad \forall i, w \tag{13}$$

$$0 \le P_{CH\ i,\tau,w} \le CR_i \quad \forall i, \tau, w \tag{14}$$

$$0 \le P_{DCH\ i,\tau,w} \le DR_i \quad \forall i, \tau, w \tag{15}$$

$$E_i^{lo} \le E_i^{in} + \sum_{o=1}^{\tau} \left(\eta_i^{CH} P_{CH\ i,o,w} - \frac{1}{\eta_i^{DCH}} P_{DCH\ i,o,w} \right) \le E_i^{up} \quad \forall i, \tau, w \tag{16}$$

$$P_{CVE\ i,\tau,w} = P_{VPP\ i,\tau,w} + P_{LO\ i,\tau,w} \quad \forall i, \tau, w \tag{17}$$

$$P_{LO\ i,\tau,w} = \alpha_i |P_{CVE\ i,\tau,w}| + \beta_i |Q_{CVE\ i,\tau,w}| \quad \forall i, \tau, w \tag{18}$$

$$\sqrt{\left(P_{CVE\ i,\tau,w}\right)^2 + \left(Q_{CVE\ i,\tau,w}\right)^2} \le S_{CVE\ i}^{up} \quad \forall i, \tau, w \tag{19}$$

In Eq. (1) the objective function of the operation problem of SDN with CVEs is formulated. This equation represents the maximization of expected CVEs profits in the energy market (the first part of Eq. (1)) and the reactive power market (the second part of Eq. (1)) [6]. Profit in each market equals the multiplications of the market price and power of the CVEs associated with that market. If the CVEs have a positive value, it means that they are making a profit from the relevant market. However, if the CVEs have a negative value, it means that they are purchasing from the relevant market, and Eq. (1) in this case represents the cost. In addition, based on [6], the reactive power price was considered as a ratio (K_Q) of the energy price.

The AC-OPF limits in SDN are expressed in Eqs. (2)-(9) [13], [14], [17], [18]. Eqs. (2)-(6) represent the AC-PF equation [30], [31], which shows active and reactive power balance in SDN buses, active and reactive power across the distribution line, and the voltage angle of the slack bus [13], [14]. Eqs. (7)-(9) represent the operating limits of the SDN, which denote the maximum apparent power limit across the distribution line and distribution substation, and the bus voltage limit R28, respectively [17], [18]. As per the equations, a distribution substation located on the slack bus connects the SDN to the upstream network. Thus, the P_{DS} and Q_{DS} variables in other buses have a value of zero, and Eq. (8) is expressed only for the slack bus. In the context of Eq. (9), its upper limit is to prevent equipment insulation failure because of overvoltage, and the lower limit is to prevent power outages caused by high voltage drop [18]. Moreover, it is assumed in the problem that there are two types of critical and non-critical loads. Critical loads are placed on buses whose voltage amplitude changes are not significant. Therefore, in these buses, the voltage amplitude is generally maintained in the range of [0.98 1.02] [11]. In non-critical loads, a wider range of voltage amplitude can be tolerated, so that in these conditions the voltage amplitude range is generally [0.9 1.05] [11]. The network flexibility constraint has been presented in Eq. (10). In this constraint, the parameter α_F represents flexibility tolerance, and if its value tends to zero, then 100% flexibility is obtained. It is noted that there is uncertainty in generated active power of RESs, therefore there will be different values for active power in different scenarios. Thus, the flexible sources such as storage and responsive loads which are able to control active power, can compensate for the power fluctuation of RESs in network. This leads that network being able to inject a certain amount of active power in each scenario, which means a high flexibility of network [11]. Eq. (10) can be used to address this issue.

The operation model of CVEs is stated in Eqs. (11)-(19). In these constraints, Eqs. (11)-(16) relate to the formulation of VPPs. As provided in Eq. (11) of power balance in VPP. Then, the DRP operation model is presented in Eqs. (12)-(13). This DRP is an incentive model based on energy prices. In this DRP, consumers shift part of their energy demand from expensive periods to cheap intervals. Since expensive (cheap) energy hours generally correspond to the peak (off-peak) period [13], consumers in this DRP provide a percentage of energy consumption required during peak hours during off-peak hours. Thus, Eq. (12) indicates the extensive of variations in active power in the DRP, and Eq. (13) guarantees that the total energy demand during peak times is provided during off-peak periods [13]. The operation model of storage devices is expressed in Eqs. (14)-(16) [1], [32]. These equations represent the boundaries of charge and discharge rates, respectively, and the limits of the energy stored in the storage. In stationary storage devices such as batteries; charge and discharge rates, CR and DR; initial energy, E^{in}; and the minimum and maximum storable energy in storage, E^{lo} and E^{up}, are independent of time and scenario [13]. However, in mobile storage devices such as EVs, these parameters change over time and scenario, because the number of EVs changes at any moment and scenario [33], [34]. Hence, in the operating model of EVs, these parameters will have an index of τ and w. EVs must also store a certain amount of energy during the day. In this paper, it is assumed that EVs tend to fully charge their batteries [34]. Accordingly, Eq. (16) for EVs is modeled as Eq. (20). Note that at moment τ and w, the CR, DR, and E^{lo} for EVs equals the sum of the charge rate, discharge rate, and minimum energy of the EVs integrated with the network at this time, respectively. The value of E^{in} at moment τ is equal to the total initial energy of the recently-connected EVs at moment τ. The value of E^{up} at moment τ and w equals the sum of energy demand of the EVs disconnected from the network at that moment. Considering the full charge for each EV, its power consumption will be equal to its battery capacity [34]. The following is the formulation of ES in Eqs. (17)-(19). Note that P_{CEV} is on the SDN side, P_{VPP} is on the VPP output side. Therefore, between these two powers, there are ES losses. So, the active power of CVE as Eq. (17) will be equal to the sum of the active power

of VPP and the active losses of ES. In Eq. (18), the ES loss is calculated, which is a factor of the absolute value of the active and reactive power of CVE [11]. Finally, the ES capacity limit is presented in Eq. (19), which represents the maximum apparent power flowing through the ES. Also note that, as in Fig. 1, there is a controllable load at the ES output, which is used for voltage regulation. In this paper, as in [11], it is modeled as an impedance, current, and constant power (ZIP) load, which appears to the left of Eqs. (2) and (3). Finally, the expressions λ and μ represent the dual variables of different constraints.

$$E^{lo}_{i,\tau,w} \leq E^{in}_{i,\tau,w} + \sum_{\sigma=1}^{\tau}\left(\eta^{CH}_i P_{CH\ i,o,w} - \frac{1}{\eta^{DCH}_i} P_{DCH\ i,o,w}\right) = E^{up}_{i,\tau,w} \quad \forall i,\tau,w \tag{20}$$

The proposed scheme includes an optimization model. Optimization formulation contains objective function [35], [36], [37], [38], [39], [40], [41], [42] and constraints [43], [44], [45], [46], [47], [48], [49], [50], [51], [52], [53]. To apply the optimization problem on the distribution network, the grid needs to smart devices [54], [55], [56], [57], [58] and Telecommunications equipment [59], [60].

B. LINEAR APPROXIMATION MODEL

Eqs. (1)-(19) is in the form of non-convex nonlinear programming (NLP) (due to AC-PF constraints [1], [2]). Solvers of this problem generally do not have the same solutions [6], so the coefficient of confidence in response to this problem is low. This formulation is also an operation problem. In operation problems, the execution step is generally small, thus the low calculation time is of particular importance in these problems [6]. However, NLP solvers work based on iterative approaches, which are time-demanding [1]. Therefore, a linear approximation model (LAM) is extracted for the proposed scheme because its solvers are able to find a unique solution shortly [13].

To linearize AC-OPF constraints, it should be noted that according to [6], the voltage angle deviation at the two sending and receiving end buses of a distribution line for a distribution network is generally less than 6 degrees. Therefore, the expressions $\cos(\sigma_{b,\tau,w} - \sigma_{k,\tau,w})$ and $\sin(\sigma_{b,\tau,w} - \sigma_{k,\tau,w})$ are approximated to 1 and $(\sigma_{b,\tau,w} - \sigma_{k,\tau,w})$, respectively. Also, to linearize the expression of the squared voltage amplitude and the product of the voltage amplitudes, the conventional piecewise linearization technique is used. In this method, the variable V is expressed as $\sum_j \Delta V_j$ where ΔV and j represent the voltage deviation and the piecewise index, respectively. In this case, based on [13], V^2 is formulated as $(V^{\mathrm{lo}})^2 + \sum_j sl_j \Delta V_j$, and $V_b V_k$ will be equal to $(V^{\mathrm{lo}})^2 + V^{\mathrm{lo}} \sum_j (\Delta V_{b,j} + \Delta V_{k,j})$. So, the variable ΔV replaces the variable V in AC-OPF, whose maximum value is equal to the ratio between the difference between V^{lo} and V^{up} to the number of linear pieces (n_J). Therefore, the linearized formulation of constraints (2)-(5) and (9) can be written as Eqs. (21)-(25), respectively. With AC-OPF linearization, it is known as linearized AC-OPF (LAC-OPF).

$$P_{DS\ b,\tau,w} + P_{PV\ b,\tau,w} + P_{WT\ b,\tau,w} + \sum_i A_{i,b} P_{CVE\ i,\tau,w} - \sum_k B_{b,k} P_{DL\ b,k,\tau,w} = (1 - C_b) P_{L\ b,\tau,w} + C_b P_{L\ b,\tau,w} \left(\begin{array}{l} Z\left(\frac{(V^{lo}_b)^2 + \sum_j sl_j \Delta V_{b,\tau,w,j}}{\left(V^{LF}_{b,\tau,w}\right)^2}\right) + \\ I\left(\frac{\sum_j \Delta V_{b,\tau,w,j}}{V^{LF}_{b,\tau,w}}\right) + P \end{array} \right) \quad \forall b,\tau,w \tag{21}$$

$$Q_{DS\ b,\tau,w} + \sum_i A_{i,b} Q_{CVE\ i,\tau,w} - \sum_k B_{b,k} Q_{DL\ b,k,\tau,w} = (1 - C_b) Q_{L\ b,\tau,w} + C_b Q_{L\ b,\tau,w} \left(\begin{array}{l} Z\left(\frac{(V^{lo}_b)^2 + \sum_j sl_j \Delta V_{b,\tau,w,j}}{\left(V^{LF}_{b,\tau,w}\right)^2}\right) + \\ I\left(\frac{\sum_j \Delta V_{b,\tau,w,j}}{V^{LF}_{b,\tau,w}}\right) + P \end{array} \right) \quad \forall b,\tau,w \tag{22}$$

$$P_{DL\ b,k,\tau,w} = g_{DL\ b,k} \sum_j \left(\left(sl_j - V^{lo}_b\right) \Delta V_{b,\tau,w,j} - V^{lo}_b \Delta V_{k,\tau,w,j} \right) - \left(V^{lo}_b\right)^2 b_{DL\ b,k} \left(\sigma_{b,\tau,w} - \sigma_{k,\tau,w}\right) \quad \forall b,k,\tau,w \tag{23}$$

$$Q_{DL\ b,k,\tau,w} = -g_{DL\ b,k} \sum_j \left(\left(sl_j - V^{lo}_b\right) \Delta V_{b,\tau,w,j} - V^{lo}_b \Delta V_{k,\tau,w,j} \right) - \left(V^{lo}_b\right)^2 g_{DL\ b,k} \left(\sigma_{b,\tau,w} - \sigma_{k,\tau,w}\right) \quad \forall b,k,\tau,w \tag{24}$$

$$0 \leq \Delta V_{b,\tau,w,j} \leq \frac{V^{up}_b - V^{lo}_b}{n_J} \quad \forall b,\tau,w,j \tag{25}$$

Eqs. (7)-(8) and Eq. (19) are a circular plane with the center of origin and the radius S in PQ coordinates, i.e., $\sqrt{P^2 + Q^2}$.To linearize this equation, a circular plane is approximated to a plane in the form of a regular polygon with n_P sides [6]. Each side of this plane has a linear relationship in the form of $P \times \cos(\omega \times \Delta\sigma) + Q \times \sin(\omega \times \Delta\sigma) = S$ [6]. In this equation, ω represents the side that varies between 1 and n_P. Also, indicates an angle deviation of $\frac{360}{n_P}$. Next, from each side, a square plate can be extracted as $P \times \cos(\omega \times \Delta\sigma) + Q \times \sin(\omega \times \Delta\sigma) \leq S$; considering the planes from all sides in the proposed problem, a plate is extracted in the form of a regular polygon [13]. Therefore, Eqs. (7)-(8) and Eq. (19) are linearized as Eqs. (26)-(28), respectively.

$$P_{DL\ b,k,\tau,w} \cos(\omega \times \Delta\delta) + Q_{DL\ b,k,\tau,w} \sin(\omega \times \Delta\delta) \leq S^{up}_{DL\ b,k} \quad \forall b,k,\tau,w,\omega \tag{26}$$

$$P_{DS\ b,\tau,w} \cos(\omega \times \Delta\delta) + Q_{DS\ b,\tau,w} \sin(\omega \times \Delta\delta)$$

$$\leq S^{up}_{DS\ b} \quad \forall b = \text{Slack bus}, \tau, w, \omega \tag{27}$$

$$P_{CVE\ i,\tau,w}\cos(\omega \times \Delta\delta) + Q_{CVE\ i,\tau,w}\sin(\omega \times \Delta\delta) \leq S^{up}_{CVE\ i} \quad \forall i, \tau, w, \omega \tag{28}$$

In Eq. (18), the nonlinear expression is the resultant of the active and reactive power of the CVE. Since the distribution network generally has an ohmic-inductive load, the CVE is expected to operate to control reactive power in capacitive mode (reactive power generation). Hence, the phrase $|Q_{\text{CVE}}|$ will be Q_{CVE}. Yet, to linearize $|P_{\text{CEV}}|$, the variable P_{CVE} is first divided into positive (P^{+}_{CVE}) and negative (P^{-}_{CVE}) components, which have positive values and contain the positive and negative values of the P_{CVE} variable, respectively. As a result, P_{CVE} is equal to the difference of P^{+}_{CVE} and P^{-}_{CVE}, and $|P_{\text{CEV}}|$ equals the sum of the positive and negative components of active power of CVE. Accordingly, Eq. (18) is linearized as Eqs. (29)-(31), where Eq. (29) represents the linearized model of Eq. (18). In Eq. (29), PCVE is expressed in terms of positive and negative components. The limitations of these components are also stated in Eqs. (30) and (31).

$$P_{LO\ i,\tau,w} = \alpha_i \left(P^{+}_{CVE\ i,\tau,w} + P^{-}_{CVE\ i,\tau,w}\right) + \beta_i Q_{CVE\ i,\tau,w} \quad \forall i, \tau, w \tag{29}$$

$$P_{CVE\ i,\tau,w} = P^{+}_{CVE\ i,\tau,w} - P^{-}_{CVE\ i,\tau,w} \quad \forall i, \tau, w \tag{30}$$

$$0 \leq P^{+}_{CVE\ i,\tau,w} \leq S^{up}_{CVE\ i} \quad \forall i, \tau, w \tag{31}$$

$$0 \leq P^{-}_{CVE\ i,\tau,w} \leq S^{up}_{CVE\ i} \quad \forall i, \tau, w \tag{32}$$

Finally, the linearized model of the suggested scheme can be stated as Eqs. (33)-(34):

$$\max \quad F = \sum_{i,\tau,w} \pi_w \rho_{E\ \tau,w} \left(P_{CVE\ i,\tau,w} + K_Q Q_{CVE\ i,\tau,w}\right) \tag{33}$$

subject to:

$$Eqs\ 6, 10-17, \text{ and } 21-31 \tag{34}$$

III. UNCERTAINTY MODELLING

Parameters of load, P_L and Q_L; renewable power, P_{PV} and Q_{WT}; energy price, ρ_E; charge and discharge rates of EVs, CR and DR; initial energy of EVs, E^{in}; minimum and maximum stored energy in EVs, E^{lo} and E^{up}; are uncertainty parameters. Thus, stochastic programming based on the hybrid Monte Carlo Simulation (MCS) method and Kantorovich technique have been adopted to provide a modeling of these parameters [14]. To this end, first, the MCS generates many scenarios based on the normal PDF for power demand and energy price [61], beta/Weibull PDFs for solar/wind type RES [62], and Rayleigh PDF for EV parameters [63]. Moreover, the PDF of uncertainties specifies the mean and standard deviation. After that, the probability of each generated scenario (π^0) can be found by multiplying the probability of uncertainties in this scenario. Next, the Kantorovich method selects several scenarios that are more probable to happen. In this case, the probability of scenario s obtained from the Kantorovich method (π_w) is equal to $\frac{\pi^0_w}{\sum_w \pi^0_w}$ so that $\sum_w \pi_w = 1$. Ref. [14] provides more details about the proposed approach.

IV. NUMERICAL RESULTS AND DISCUSION

A. CASE STUDY

The scheme suggested in this section is applied to the IEEE 69-bus radial SDN [13] as shown in Fig. 2. This network has 1 MVA base power and 12.66 kV base voltage. The allowable voltage range for non-critical (critical) loads is [0.9 1.05] ([0.98 1.02]) per-unit (p.u.) [11]. The locations of critical loads in this network are buses 30-32, 49, 8-9, and 41-44. Other buses have non-critical loads. Information about distribution lines and substations along with peak load data are available in [13]. The daily load profile can be obtained by multiplying the peak load and the daily load factor curve (Fig. 3) [1]. Energy prices for the three off-peak (1:00-7:00), medium load (8:00-16:00 and 23:00-00:00), and peak (17:00-22:00) periods is 16 \$/MWh, 24 \$/MWh, and 30 \$/MWh, respectively [1]. K_Q is assumed to be 8% based on [6]. The network has renewable sources such as WTs and PVs. WTs with a size of 0.5 MW are installed at buses 17 and 49, and PVs with a size of 0.5 MW are installed at buses 41 and 53. The daily profile of their active generating power is equal to the product of their capacity and the daily curve of their generating power rate (Fig. 3) [13]. In addition, there are up to 7 flexible-renewable VPPs in the network, abbreviated FRVPP. These FRVPPs contain renewable sources as well as flexibility sources (storage and responsive loads). The locations of FRVPPs are shown in Fig. 2. These FRVPPs are connected to the network by ES and form a CVE. The loads on the connecting buses of CVEs are assumed to be controllable, hence the ZIP load is used on these buses. In the ZIP load model, the coefficients Z, I, and P have values of 0.3, 0.3, and 0.4, respectively [11]. Loss coefficients of ES, i.e., α and β, are 0.09 and 0.075, respectively [6]. Each ES also has a capacity of 5 MVA. The active peak load per FRVPP is 200 kW. Each FRVPP has WT, PV, batteries, EVs, and responsive loads. The capacity of WTs and PVs in FRVPPs 1, 2, 6, and 7 is equal to 0.3 MW, but in other FRVPPs, it is equal to 0.5 MW. FRVPPs 1, 2, 6, and 7 each have up to 150 EVs, but other FRVPPs each have up to 200 EVs. The number of EVs per moment equals the multiplication of the number of EVs per FRVPP and the daily EV penetration rate curve (Fig. 3) [6]. Other characteristics of EVs such as charge/discharge rate, charge/discharge efficiency, battery size, initial energy, and minimum energy storage in the battery are stated in [6] and [34]. Consumers at each FRVPP participate in DRP at a rate of 50%. There is a battery with a capacity of 1 MWh per FRVPP, where the minimum energy stored in it and its initial energy are 10% of the battery capacity. The charging and discharging rate of the battery is 0.5 MW, and the charging and discharging efficiency is 92%. To achieve high flexibility in the network, the flexibility tolerance is considered to 0.05 p.u. Also, in the stochastic

TABLE 2. Convergence status of the scheme obtained by different solvers in α_F= 0.05 p.u.

Model	Algorithm	Objective function ($)	convergence iteration	Calculation time (s)
NLP	IPOPT	989.1	273	891.7
	CONOPT	935.2	354	1008
	DISOPT	Infeasible	Infeasible	Infeasible
	BARON	902.5	385	1261
LAM	CPLEX	1032.4	39	19.8
	CONOPT	1032.4	41	24.3
	BDMLP	1032.4	79	27.9

optimization, MCS generates 1000 scenario samples, then, the Kantorovich method selects 60 scenario samples from generated scenarios.

B. RESULTS AND DISCUSSIONS

Here, we simulate the suggested approach in accordance with the data of sub-section IV-A in the GMAS software [64]. For the linear model Eqs. (31)-(33), the circular plane is approximated to a plane in the form of a regular 90-gon. Also, in the conventional piecewise linearization technique, 5 linear pieces are used.

noitemsep,nolistsep

- Evaluation of the convergence status of the proposed scheme: Table 2 reports the convergence status of the stochastic problem in two NLP Eqs. (1)-(19) and LAM Eqs. (31)-(33) models for different solvers at flexibility tolerance of 0.05 p.u. In the NLP model, IPOPT, CONOPT, DISOPT, and BARON solvers [64] are used to solve the problem. Among these algorithms, DISOPT is not able to achieve the optimal solution. Other algorithms do not have a unique optimal solution so IPOPT has a better situation than other solvers because it has a more optimal point (maximum objective function or F) and higher convergence speed (lower convergence iteration (CI) and lower computational time (CT)) than other algorithms. CPLEX, CONOPT, and BDMLP algorithms are used to solve the linear problem [64]. These algorithms succeed to reach a unique solution. The difference is in CI and CT, which makes CPLEX more suitable because its convergence speed is the highest (minimum CI and CT). Therefore, the CPLEX solver has been employed to find a solution to the problem. Concerning calculation time, the nonlinear IPOPT-based model has a CT of 891.7 s. But in the CPLEX-based linear model, it has been reduced to about 19.8 s. That is, CT in the linear model is reduced by about 97.8% compared to the nonlinear model. Therefore, the CPLEX algorithm is in a good position compared to other models and solvers, because it has a unique optimal solution and considerably low computational time. Finally, the computational error of the power and voltage variables in the linear model compared to the main formulation based on the nonlinear model is reported in Table 3 for α_F= 0.05 p.u. The computational error of active and reactive power is about 2%, but it is about 0.3-0.45% for voltage. Computational time in the linear method is very low, which corresponds to the operation goals in the operation problems, the computational errors in this regard can be ignored.
- Evaluation of the performance of VPPs in CVEs: Fig. 4 illustrates he predicted daily curve of the total active power of VPPs and its devices for α_F= 0.05 p.u. as is observed in Fig. 4(a), the daily active power curve of WTs and PVs is the same as the daily power rate curve of their output in Fig. 3. The reason is that, according to sub-section IV-A, the active power generation of a renewable source equals the multiplication of its size and the generation power of the mentioned source. Fig. 4(a) depicts the daily curve of the active power of storage devices, i.e., stationary (batteries) and mobile (EVs) storage, and the responsive loads. As is seen, storage and responsive loads operate generally at low energy price hours (1:00-16:00 and 23:00-00:00) corresponding to the off-peak and medium load intervals in the charge mode or in the mode of receiving energy from VPPs. However, at high energy price hours (17:00-22:00) corresponding to the peak load period, they operate in the mode of discharging or injecting energy into the VPPs. In Fig. 4(a), the EVs perform two charging operations. Once to supply the energy they need to travel, which has a high energy level and appears between 1:00-7:00 and 23:00-00:00. The other is when they are charged from 12:00-16:00 until they inject the stored energy of the EV batteries into the VPPs or SDNs during the peak load period. This trend of performance of storage devices and responsive loads aims to gain high financial profit in the energy market. For example, batteries purchase 6.3 MWh (7 hours$\times$0.9 MW according to Fig. 4(a)) energy at 16 \$/MWh during 1:00-7:00 from SDN. Nonetheless, they sell the same amount of energy to SDN during peak hours at 30 \$/MWh. Therefore, it is expected that the operation of these batteries will increase the financial benefit of CVEs in the energy market.

  It is noteworthy that in the flexibility discussion, as given in Eq. (10), the goal is for CVEs to minimize power swings of renewable sources in the different scenarios in comparison to the scenario related to the deterministic model. According to Fig. 4(a), since renewable sources have active generation capacity at all hours, it is expected that CVEs will operate at all hours for flexibility. Hence, the flexibility sources in CVEs, such as storage devices and responsive loads, are operating at most hours. Fig. 4(b) depicts the daily active power curve of VPPs, which depends on the performance of renewables, storage devices, responsive loads, and passive load based on Eq. (11). Finally, using this figure, it can be seen that VPPs are in energy consumption mode during off-peak periods, 1:00-7:00, because during these hours, storage devices and responsive loads according to Fig. 4(a) are in the charging mode. However, at other hours, VPPs appear as power generators in the SDN.

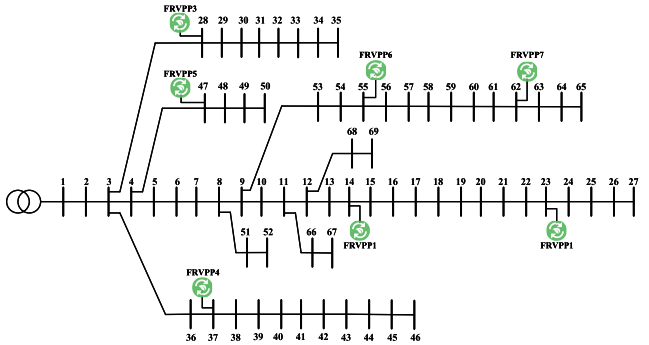

FIGURE 2. The 69-bus SDN in the presence of FRVPPs [13].

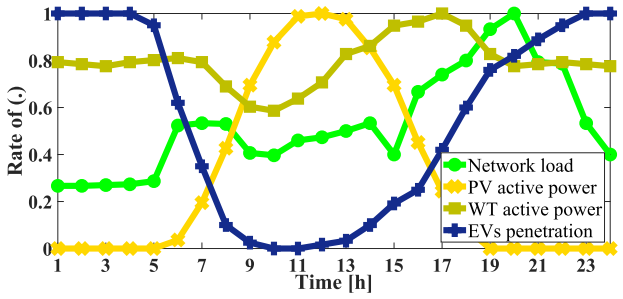

FIGURE 3. The daily curve of RESs power rate [13], load factor [1], and EVs penetration rate.

TABLE 3. Calculation error of different variables in linear model comparison to original non-linear model in $\alpha_F = 0.05$ p.u.

Model	LAM	NLP	Computational error (%)
Algorithm	CPLEX	IPOPT	
Active power of distribution post at 20:00 (p.u.)	1.99	2.03	1.97
Reactive power of distribution post at 20:00 (p.u.)	1.302	1.324	1.66
Mean of voltage amplitude (p.u.)	0.960	0.957	0.31
Mean value of voltage angle (p.u.)	-0.0452	-0.0450	0.44

- Assessing the operation and economic status of CVEs in SDN: Predicted daily curve of active and reactive power of CVEs along with the CVEs' profit in energy and reactive power markets for $\alpha_F = 0.05$ p.u. are drawn in Fig. 5.

  The daily active power curve of the CVEs is shown in Fig. 5(a), the trend of which is the same as that of the active power of VPPs in Fig. 4(b). This is because, according to Eq. (17), the active power of CVEs equals the sum of the active power of VPPs and ES losses. Since the coefficients α and β are less than 0.1 according to sub-section IV-A, the effect of the active power of VPPs is much greater than the effect of ES losses on the active power of CVEs. Therefore, the curve of variations in active power of CVEs will be close to that of the active power of VPPs. Fig. 5(a) shows the daily reactive power curve of CVEs. According to this figure, the maximum reactive power of CVEs injected into SDN appeared during 1:00-7:00 because VPPs are in consumer mode at this time and receive significant active power from SDN. Therefore, to prevent high voltage drop, CVEs provide high reactive power into SDN during these hours. At other times, CVEs inject high active power into the SDN as shown in Fig. 5(a). Therefore, to prevent overvoltage in the SDN, CVEs inject low reactive power into the SDN during these hours. However, in these intervals, the increase in reactive power of CVEs in the peak load interval is due to the increase in load in this interval based on the daily load factor curve in Fig. 3. The daily profit curve of CVEs in the energy and ancillary services (or reactive power) markets is plotted in Fig. 5(b), the trend of changes of which is very similar to that of the active power of CVEs. This is due to the very low reactive power price compared to the energy price based on sub-section IV-A. Therefore, this issue has made an impact on the energy market on the profits of CVEs more than on the ancillary services market. The benefit of CVEs and the cost of modeling uncertainty for the deterministic and stochastic models of the proposed plan are presented in Table 4. There is only one scenario in the deterministic model that contains the expected values of the uncertainty parameters. The cost of modeling uncertainty equals the difference between the objective function (Eq. (1)) (profit of CVEs) in deterministic and stochastic models. Due to the inclusion of expected uncertainty values in the scenario of the deterministic model, it is impossible to evaluate the flexibility of the proposed design. In contrast, the quantity of the objective function for various values of flexibility tolerance is reported in Table 4 for the stochastic model. According to this table, the increase in flexibility tolerance (corresponding to the decrease in the importance of flexibility based on Eq. (10)) results in a rise in the profit of CVEs because, in order to increase flexibility based on Fig. 4(a), the flexibility resources must be active at all times and compensate the power fluctuations of RESs in various scenarios. However, if the value of flexibility decreases, the flexibility resources can be switched off in some hours. For instance, if flexibility is not incorporated into the proposed plan ($\alpha_F \longrightarrow \infty$), flexible sources such as storages will only charge (discharge) during times when energy prices are low (high). Consequently, they are off during mid-peak hours and do not incur any costs for CVEs during this time. Therefore, the value of CVEs increases as the value of flexibility decreases. Moreover, according to Table 4, uncertainty modeling in stochastic optimization as compared to the deterministic model reduces the profit of CVEs. The difference between this profit in two deterministic and stochastic models is considered the cost of modeling uncertainties. In the deterministic model, the benefit of CVEs does not depend on flexibility and has a fixed value. However, in the stochastic model, as the flexibility tolerance increases, so does the benefit of CVEs, which corresponds to a decrease in the cost of uncertainty modeling. However, under the condition of total flexibility, or 100% ($\alpha_F = 0$), the cost of modeling uncertainties

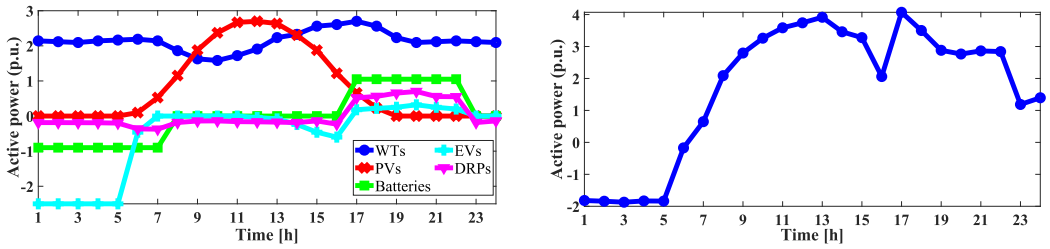

(a) RESs, storages and DRPs (b) VPPs

FIGURE 4. Expected daily active power curve of, a) RESs, storages and DRPs, b) VPPs in the α_F= 0.05 p.u.

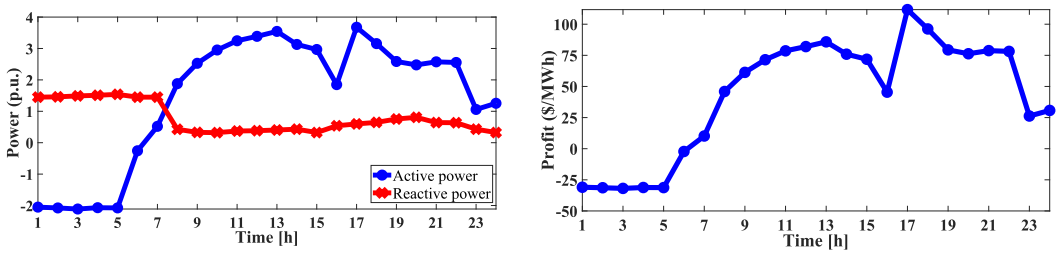

(a) active and reactive power (b) profit of CVEs

FIGURE 5. Expected daily curve of, a) active and reactive power, b) profit of CVEs at α_F= 0.05 p.u.

TABLE 4. Values of economic indicators for different uncertainty modeling and values of flexibility tolerance.

Uncertainty modeling	Deterministic	Stochastic		
		α_F= 0.1	α_F= 0.05	α_F= 0.05
CVEs profit ($)	1218.6	1067.1	1032.4	1019.3
Uncertainty modeling cost ($)	-	151.5	186.2	199.3

TABLE 5. Values of operation indicators for different cases and values of flexibility tolerance.

Index	CS1	CS2		
		α_F= 0.1	α_F= 0.05	α_F= 0
EL (MWh)	2.299	1.582	1.768	1.925
MVD (p.u.) for non-critical load bus	0.092	0.046	0.047	0.049
MOV (p.u.) for non-critical load bus	0	0.010	0.008	0.007
MVD (p.u.) for critical load bus	0.088	0.02	0.02	0.02
MOV (p.u.) for critical load bus	0	0.004	0.002	0.002

is approximately 19.6% (199.3/1019.3). However, this quantity decreases as the value of flexibility declines.

- Assessment of SDN operation status: Table 4 reports the values of operation indicators including energy losses (EL), maximum voltage drop (MVD), and maximum overvoltage (MOV) in buses without/with critical loads for different flexibility tolerance for two cases: noitemsep,nolistsep
  - Case study 1 (**CS1**): Power flow studies
  - Case study 2 (**CS2**): Proposed scheme

Table 4 shows that the network without CVEs (**CS1**) has high energy loss and voltage drop. Also, in buses with critical load, the voltage drop exceeds its permissible limit of 0.02 (1-0.98). Hence, critical loads will be off with high probability in these conditions. However, in this case study, overvoltage is zero because there is no power source in the network to establish a situation with overvoltage by injecting its power into the network. In the proposed scheme (**CS2**), the status of energy loss and voltage drop becomes better compared to that of **CS1**. In other words, in the case of 100% flexibility (α_F= 0), energy loss in the SDN reduces about 16.3% $\frac{(2.299-1.925)}{2.299}$ by optimal energy management of CVEs compared with **CS1** as shown in Fig. 5. Moreover, in **CS2** for α_F= 0, the maximum voltage drop in buses without critical load decreases roughly 46.7% compared to **CS1**. This index has 0.02 p.u. increase in buses with critical load, which is about 97.7% improvement compared with **CS1**. This happens for maximum overvoltage of 0.007, but its value is less than its allowed value of 0.05 (1.05-1) p.u. In addition, based on Table 4, with decreasing the importance of flexibility in the SDN (a reduction in α_F), the amount of improvement in operation indices increases. This is due to the performance of power sources, storage, and responsive loads in accordance with the operation status enhancement. For example, in the absence of flexibility, the storage and responsive loads will be in the charging mode during the period with inexpensive energy price, i.e. 1:00-7:00. In these conditions, based on Eq. (1), more profit will be earned for CVEs and energy loss and voltage drop decreases.

V. CONCLUSION

This paper presents the operation problem of an SDN in the presence of CVE systems. CVEs participate in energy and reactive power markets, in which VPP is in an aggregating

format for power sources, storage devices, and responsive loads. The model of the suggested design is responsible for maximizing the profit of CVEs in the energy and reactive power markets by observing the AC-OPF constraints and flexibility limit of SDN and the operation model of CVEs. Then, a linear approximation model was derived for this scheme, and stochastic optimization was adopted to model the uncertainties of load, energy prices, renewable power, and energy consumption of mobile storage devices. Finally, numerical results showed that the linear algorithm can extract a unique optimal solution for the scheme. The computational time of CPLEX is much lower than that of the nonlinear model of the proposed scheme, and the computational error of 2% and 0.4% for power and voltage in this algorithm, respectively, compared to the original nonlinear model of the proposed scheme can be ignored with respect to computational time. Then, with the optimal operation of power sources, responsive loads, and storage in the form of VPP, CVEs were consumers (producers) of energy in off-peak (medium and peak) load periods. CVEs generated high reactive power during the off-peak period compared to other hours to prevent voltage drop due to the energy consumption of CVEs during this interval. Ultimately, this performance of CVEs has led them to receive financial benefits in most of the operating hours of these markets. In the 100% flexibility condition, the suggested approach was able to reduce energy losses and maximum voltage drop in buses with non-critical load by about 16.3% and 46.7%, respectively in comparison with power flow studies. It also increased the maximum voltage drop across buses with critical load to the permissible value of 0.02 p.u., whereas in power flow studies it had a value greater than 0.02 p.u. Also, modeling of the uncertainties leads to a reduction of 19.6% in the CVEs profit in the mentioned markers compared to the proposed deterministic model. In the proposed plan, the scenario-based stochastic optimization is used to model the uncertainties. This method requires a significant number of scenarios to reach a reliable solution, which leads to an increase in the volume of the problem. Nonetheless, in operation problems, due to the low execution step, low computing time is of particular importance, which may not be achieved in stochastic optimization. To compensate for this issue, the use of robust optimization can be effective, which is suggested as a future work. Also, the risk caused by uncertainties is not included in the proposed plan. Therefore, the suggested scheme based on the risk model is considered as a future study.

REFERENCES

[1] M. AkbaiZadeh, T. Niknam, and A. Kavousi-Fard, "Adaptive robust optimization for the energy management of the grid-connected energy hubs based on hybrid meta-heuristic algorithm," *Energy*, vol. 235, Nov. 2021, Art. no. 121171.

[2] *Flexibility and Aggregation Requirements for Their Interaction in the Market*, Eurelectric, Brussels, Belgium, 2014.

[3] D. Wang, J. Qiu, L. Reedman, K. Meng, and L. L. Lai, "Two-stage energy management for networked microgrids with high renewable penetration," *Appl. Energy*, vol. 226, pp. 39–48, Sep. 2018.

[4] J. F. Venegas-Zarama, J. I. Muñoz-Hernandez, L. Baringo, P. Diaz-Cachinero, and I. De Domingo-Mondejar, "A review of the evolution and main roles of virtual power plants as key stakeholders in power systems," *IEEE Access*, vol. 10, pp. 47937–47964, 2022.

[5] T. Yang, K.-T. Mok, S.-C. Tan, C. K. Lee, and S. Y. Hui, "Electric springs with coordinated battery management for reducing voltage and frequency fluctuations in microgrids," *IEEE Trans. Smart Grid*, vol. 9, no. 3, pp. 1943–1952, May 2018.

[6] H. Kiani, K. Hesami, A. Azarhooshang, S. Pirouzi, and S. Safaee, "Adaptive robust operation of the active distribution network including renewable and flexible sources," *Sustain. Energy, Grids Netw.*, vol. 26, Jun. 2021, Art. no. 100476.

[7] S. E. Ahmadi, S. M. Kazemi-Razi, M. Marzband, A. Ikpehai, and A. Abusorrah, "Multi-objective stochastic techno-economic-environmental optimization of distribution networks with G2V and V2G systems," *Electric Power Syst. Res.*, vol. 218, May 2023, Art. no. 109195.

[8] A. Azarhooshang, D. Sedighizadeh, and M. Sedighizadeh, "Two-stage stochastic operation considering day-ahead and real-time scheduling of microgrids with high renewable energy sources and electric vehicles based on multi-layer energy management system," *Electr. Power Syst. Res.*, vol. 201, Dec. 2021, Art. no. 107527.

[9] M. Roustaee and A. Kazemi, "Multi-objective stochastic operation of multi-microgrids constrained to system reliability and clean energy based on energy management system," *Electr. Power Syst. Res.*, vol. 194, May 2021, Art. no. 106970.

[10] M. Roustaee and A. Kazemi, "Multi-objective energy management strategy of unbalanced multi-microgrids considering technical and economic situations," *Sustain. Energy Technol. Assessments*, vol. 47, Oct. 2021, Art. no. 101448.

[11] M. Norouzi, J. Aghaei, S. Pirouzi, T. Niknam, and M. Lehtonen, "Flexible operation of grid-connected microgrids using electric springs," *IET Gener., Transmiss. Distrib.*, vol. 14, pp. 1–10, Jan. 2020.

[12] M. Nasir, A. R. Jordehi, M. Tostado-Véliz, S. A. Mansouri, E. R. Sanseverino, and M. Marzband, "Two-stage stochastic-based scheduling of multi-energy microgrids with electric and hydrogen vehicles charging stations, considering transactions through pool market and bilateral contracts," *Int. J. Hydrogen Energy*, vol. 48, no. 61, pp. 23459–23497, Jul. 2023.

[13] S. A. F. Asl, L. Bagherzadeh, S. Pirouzi, M. Norouzi, and M. Lehtonen, "A new two-layer model for energy management in the smart distribution network containing flexi-renewable virtual power plant," *Electr. Power Syst. Res.*, vol. 194, May 2021, Art. no. 107085.

[14] J. Aghaei, M. Barani, M. Shafie-khah, A. A. Sánchez de la Nieta, and J. P. S. Catalão, "Risk-constrained offering strategy for aggregated hybrid power plant including wind power producer and demand response provider," *IEEE Trans. Sustain. Energy*, vol. 7, no. 2, pp. 513–525, Apr. 2016.

[15] R. Khalili, A. Khaledi, M. Marzband, A. F. Nematollahi, B. Vahidi, and P. Siano, "Robust multi-objective optimization for the Iranian electricity market considering green hydrogen and analyzing the performance of different demand response programs," *Appl. Energy*, vol. 334, Mar. 2023, Art. no. 120737.

[16] A. Jamali, J. Aghaei, M. Esmaili, A. Nikoobakht, T. Niknam, M. Shafie-khah, and J. P. S. Catalão, "Self-scheduling approach to coordinating wind power producers with energy storage and demand response," *IEEE Trans. Sustain. Energy*, vol. 11, no. 3, pp. 1210–1219, Jul. 2020.

[17] A. Rohani, M. Abasi, A. Beigzadeh, M. Joorabian, and G. B. Gharehpetian, "Bi-level power management strategy in harmonic-polluted active distribution network including virtual power plants," *IET Renew. Power Gener.*, vol. 15, no. 2, pp. 462–476, Feb. 2021.

[18] A. Zare Ghaleh Seyyedi, S. A. Nejati, R. Parsibenehkohal, M. Hayerikhiyavi, F. Khalafian, and P. Siano, "Bi-level sitting and sizing of flexi-renewable virtual power plants in the active distribution networks," *Int. J. Electr. Power Energy Syst.*, vol. 137, May 2022, Art. no. 107800.

[19] N. Lou, Y. Zhang, Y. Wang, Q. Liu, H. Li, Y. Sun, and Z. Guo, "Two-stage congestion management considering virtual power plant with cascade hydro-photovoltaic-pumped storage hybrid generation," *IEEE Access*, vol. 8, pp. 186335–186347, 2020.

[20] F. Ahmad, A. Iqbal, I. Asharf, M. Marzband, and I. Khan, "Placement and capacity of EV charging stations by considering uncertainties with energy management strategies," *IEEE Trans. Ind. Appl.*, pp. 1–10, 2023.

[21] Z. Yi, Y. Xu, J. Zhou, W. Wu, and H. Sun, "Bi-level programming for optimal operation of an active distribution network with multiple virtual power plants," *IEEE Trans. Sustain. Energy*, vol. 11, no. 4, pp. 2855–2869, Oct. 2020.

[22] X. Yan, C. Gao, M. Song, T. Chen, J. Ding, M. Guo, X. Wang, and D. Abbes, "An IGDT-based day-ahead co-optimization of energy and reserve in a VPP considering multiple uncertainties," *IEEE Trans. Ind. Appl.*, vol. 58, no. 3, pp. 4037–4049, May 2022.

[23] D. Xiao, H. Chen, C. Wei, and X. Bai, "Statistical measure for risk-seeking stochastic wind power offering strategies in electricity markets," *J. Mod. Power Syst. Clean Energy*, vol. 10, no. 5, pp. 1437–1442, Sep. 2022.

[24] F. H. Aghdam, M. W. Mudiyanselage, B. Mohammadi-Ivatloo, and M. Marzband, "Optimal scheduling of multi-energy type virtual energy storage system in reconfigurable distribution networks for congestion management," *Appl. Energy*, vol. 333, Jan. 2023, Art. no. 120569.

[25] S. A. Mansouri, A. Rezaee Jordehi, M. Marzband, M. Tostado-Véliz, F. Jurado, and J. A. Aguado, "An IoT-enabled hierarchical decentralized framework for multi-energy microgrids market management in the presence of smart prosumers using a deep learning-based forecaster," *Appl. Energy*, vol. 333, Mar. 2023, Art. no. 120560.

[26] A. S. Daramola, S. E. Ahmadi, M. Marzband, and A. Ikpehai, "A cost-effective and ecological stochastic optimization for integration of distributed energy resources in energy networks considering vehicle-to-grid and combined heat and power technologies," *J. Energy Storage*, vol. 57, Jan. 2023, Art. no. 106203.

[27] K. Saberi-Beglar, K. Zare, H. Seyedi, M. Marzband, and S. Nojavan, "Risk-embedded scheduling of a CCHP integrated with electric vehicle parking lot in a residential energy hub considering flexible thermal and electrical loads," *Appl. Energy*, vol. 329, Jan. 2023, Art. no. 120265.

[28] S. E. Ahmadi, M. Marzband, A. Ikpehai, and A. Abusorrah, "Optimal stochastic scheduling of plug-in electric vehicles as mobile energy storage systems for resilience enhancement of multi-agent multi-energy networked microgrids," *J. Energy Storage*, vol. 55, Nov. 2022, Art. no. 105566.

[29] F. Ahmad, I. Ashraf, A. Iqbal, M. Marzband, and I. Khan, "A novel AI approach for optimal deployment of EV fast charging station and reliability analysis with solar based DGs in distribution network," *Energy Rep.*, vol. 8, pp. 11646–11660, Nov. 2022.

[30] A. Taghieh, A. Mohammadzadeh, C. Zhang, N. Kausar, and O. Castillo, "A type-3 fuzzy control for current sharing and voltage balancing in microgrids," *Appl. Soft Comput.*, vol. 129, Nov. 2022, Art. no. 109636.

[31] P. Li, J. Hu, L. Qiu, Y. Zhao, and B. K. Ghosh, "A distributed economic dispatch strategy for power–water networks," *IEEE Trans. Control Netw. Syst.*, vol. 9, no. 1, pp. 356–366, Mar. 2022.

[32] W. Dang, S. Liao, B. Yang, Z. Yin, M. Liu, L. Yin, and W. Zheng, "An encoder–decoder fusion battery life prediction method based on Gaussian process regression and improvement," *J. Energy Storage*, vol. 59, Mar. 2023, Art. no. 106469.

[33] F. Azam, M. H. Sabzalian, S. Pirouzi, M. Aredes, B. W. Franca, and A. C. Cunha, "Two-layer coordinated energy management method in the smart distribution network including multi-microgrid based on the hybrid flexible and securable operation strategy," *Int. Trans. Electr. Energy Syst.*, vol. 11, no. 4, pp. 2855–2869, 2022.

[34] M. R. Jokar, S. Shahmoradi, A. H. Mohammed, L. K. Foong, B. N. Le, and S. Pirouzi, "Stationary and mobile storages-based renewable off-grid system planning considering storage degradation cost based on information-gap decision theory optimization," *J. Energy Storage*, vol. 58, Feb. 2023, Art. no. 106389.

[35] L. Guo, C. Ye, Y. Ding, and P. Wang, "Allocation of centrally switched fault current limiters enabled by 5G in transmission system," *IEEE Trans. Power Del.*, vol. 36, no. 5, pp. 3231–3241, Oct. 2021.

[36] Z. Zhang, F. M. A. Altalbawy, M. Al-Bahrani, and Y. Riadi, "Regret-based multi-objective optimization of carbon capture facility in CHP-based microgrid with carbon dioxide cycling," *J. Cleaner Prod.*, vol. 384, Jan. 2023, Art. no. 135632.

[37] Y. Lin, H. Song, F. Ke, W. Yan, Z. Liu, and F. Cai, "Optimal caching scheme in D2D networks with multiple robot helpers," *Comput. Commun.*, vol. 181, pp. 132–142, Jan. 2022.

[38] J. Li, Y. Deng, W. Sun, W. Li, R. Li, Q. Li, and Z. Liu, "Resource orchestration of cloud-edge–based smart grid fault detection," *ACM Trans. Sensor Netw.*, vol. 18, no. 3, pp. 1–26, Aug. 2022.

[39] F. Yu, L. Liu, L. Xiao, K. Li, and S. Cai, "A robust and fixed-time zeroing neural dynamics for computing time-variant nonlinear equation using a novel nonlinear activation function," *Neurocomputing*, vol. 350, pp. 108–116, Jul. 2019.

[40] B. Xiong, K. Yang, J. Zhao, and K. Li, "Robust dynamic network traffic partitioning against malicious attacks," *J. Netw. Comput. Appl.*, vol. 87, pp. 20–31, Jun. 2017.

[41] W. Li, Y. Ding, Y. Yang, R. S. Sherratt, J. H. Park, and J. Wang, "Parameterized algorithms of fundamental NP-hard problems: A survey," *Hum.-Centric Comput. Inf. Sci.*, vol. 10, no. 1, pp. 1962–2192, Dec. 2020.

[42] Q. Tang, L. Chang, K. Yang, K. Wang, J. Wang, and P. K. Sharma, "Task number maximization offloading strategy seamlessly adapted to UAV scenario," *Comput. Commun.*, vol. 151, pp. 19–30, Feb. 2020.

[43] J. Chen, K. Li, K. Li, P. S. Yu, and Z. Zeng, "Dynamic planning of bicycle stations in dockless public bicycle-sharing system using gated graph neural network," *ACM Trans. Intell. Syst. Technol.*, vol. 12, no. 2, pp. 1–22, Mar. 2021.

[44] K. Li, X. Tang, and K. Li, "Energy-efficient stochastic task scheduling on heterogeneous computing systems," *IEEE Trans. Parallel Distrib. Syst.*, vol. 25, no. 11, pp. 2867–2876, Nov. 2014.

[45] K. Li, X. Tang, B. Veeravalli, and K. Li, "Scheduling precedence constrained stochastic tasks on heterogeneous cluster systems," *IEEE Trans. Comput.*, vol. 64, no. 1, pp. 191–204, Jan. 2015.

[46] S. Wang, Y. Long, R. Ruby, and X. Fu, "Clustering and power optimization in mmWave massive MIMO–NOMA systems," *Phys. Commun.*, vol. 49, Dec. 2021, Art. no. 101469.

[47] Y. Ma, Z. Guo, L. Wang, and J. Zhang, "Probabilistic life prediction for reinforced concrete structures subjected to seasonal corrosion-fatigue damage," *J. Struct. Eng.*, vol. 146, no. 7, Jul. 2020, Art. no. 04020117.

[48] M. Long and X. Xiao, "Outage performance of double-relay cooperative transmission network with energy harvesting," *Phys. Commun.*, vol. 29, pp. 261–267, Aug. 2018.

[49] Q. Tang, K. Wang, K. Yang, and Y.-S. Luo, "Congestion-balanced and welfare-maximized charging strategies for electric vehicles," *IEEE Trans. Parallel Distrib. Syst.*, vol. 31, no. 12, pp. 2882–2895, Dec. 2020.

[50] B. Lu, X. Meng, Y. Tian, M. Zhu, and R. O. Suzuki, "Thermoelectric performance using counter-flowing thermal fluids," *Int. J. Hydrogen Energy*, vol. 42, no. 32, pp. 20835–20842, Aug. 2017.

[51] X. Meng and R. O. Suzuki, "Simulation analysis of tilted polyhedron-shaped thermoelectric elements," *J. Electron. Mater.*, vol. 44, no. 6, pp. 1469–1476, 2015.

[52] S. Xu, W. Huang, D. Huang, H. Chen, Y. Chai, M. Ma, and W. X. Zheng, "A reduced-order observer-based method for simultaneous diagnosis of open-switch and current sensor faults of a grid-tied NPC inverter," *IEEE Trans. Power Electron.*, vol. 38, no. 7, pp. 9019–9032, Sep. 2023.

[53] X. Fan, G. Wei, X. Lin, X. Wang, Z. Si, X. Zhang, Q. Shao, S. Mangin, E. Fullerton, L. Jiang, and W. Zhao, "Reversible switching of interlayer exchange coupling through atomically thin VO2 via electronic state modulation," *Matter*, vol. 2, no. 6, pp. 1582–1593, Jun. 2020.

[54] J. Song, A. Mingotti, J. Zhang, L. Peretto, and H. Wen, "Fast iterative-interpolated DFT phasor estimator considering out-of-band interference," *IEEE Trans. Instrum. Meas.*, vol. 71, pp. 1–14, 2022.

[55] B. Zhou, K. Ding, J. Wang, L. Wang, P. Jin, and T. Tang, "Experimental study on the interactions between wave groups in double-wave-group focusing," *Phys. Fluids*, vol. 35, no. 3, Mar. 2023, Art. no. 037118.

[56] X. Zhang, Y. Wang, M. Yang, and G. Geng, "Toward concurrent video multicast orchestration for caching-assisted mobile networks," *IEEE Trans. Veh. Technol.*, vol. 70, no. 12, pp. 13205–13220, Dec. 2021.

[57] J. Wang, Y. Gao, C. Zhou, R. S. Sherratt, and L. Wang, "Optimal coverage multi-path scheduling scheme with multiple mobile sinks for WSNs," *Comput., Mater. Continua*, vol. 62, no. 2, pp. 695–711, 2020.

[58] Y.-S. Luo, K. Yang, Q. Tang, J. Zhang, and B. Xiong, "A multi-criteria network-aware service composition algorithm in wireless environments," *Comput. Commun.*, vol. 35, no. 15, pp. 1882–1892, Sep. 2012.

[59] Z. Liao, J. Peng, J. Huang, J. Wang, J. Wang, P. K. Sharma, and U. Ghosh, "Distributed probabilistic offloading in edge computing for 6G-enabled massive Internet of Things," *IEEE Internet Things J.*, vol. 8, no. 7, pp. 5298–5308, Apr. 2021.

[60] Z. Xu, W. Liang, K.-C. Li, J. Xu, and H. Jin, "A blockchain-based roadside unit-assisted authentication and key agreement protocol for Internet of Vehicles," *J. Parallel Distrib. Comput.*, vol. 149, pp. 29–39, Mar. 2021.

[61] E. Faraji, A. R. Abbasi, S. Nejatian, M. Zadehbagheri, and H. Parvin, "Probabilistic planning of the active and reactive power sources constrained to securable-reliable operation in reconfigurable smart distribution networks," *Electr. Power Syst. Res.*, vol. 199, Mar. 2021, Art. no. 107457.
[62] M. H. Amirioun and A. Kazemi, "A new model based on optimal scheduling of combined energy exchange modes for aggregation of electric vehicles in a residential complex," *Energy*, vol. 69, pp. 186–198, May 2014.
[63] B. Khorramdel, H. Khorramdel, J. Aghaei, A. Heidari, and V. G. Agelidis, "Voltage security considerations in optimal operation of BEVs/PHEVs integrated microgrids," *IEEE Trans. Smart Grid*, vol. 6, no. 4, pp. 1575–1587, Jul. 2015.
[64] *Generalized Algebraic Modeling Systems (GAMS)*. Accessed: Sep. 30, 2010. [Online]. Available: http://www.gams.com

MINGGUANG YAO was born in Henan, China, in 1975. He received the degree from the School of History and Culture, Shandong University, in 2009, and the Ph.D. degree in applied economics (law and finance) from Shanghai University. He is currently an Associate Professor with the Shanghai Institute of Tourism. His research interests include the tourism economy and tourism and leisure culture.

ZOHRE MORADI was born in Tehran, Iran, in 1994. She received the master's degree from Imam Khomeini International University, Iran. Her research interests include applied mathematics, MEMS/NEMS, and artificial intelligence.

SASAN PIROUZI received the B.Sc. degree in electrical engineering from Technical and Vocational University, Mashhad, Iran, in 2012, the M.Sc. degree from the Isfahan University of Technology, Isfahan, Iran, in 2014, and the Ph.D. degree from the Shiraz University of Technology (SUTECH), Shiraz, Iran, in 2017. His research interests include power system operation and planning, electric vehicles, DERs, and the application of optimization methods in power systems.

MOUSA MARZBAND (Senior Member, IEEE) is currently an Associate Professor (Reader) with the Net Zero Industry Innovation Centre, Teesside University, U.K., and also with the Center of Research Excellence in Renewable Energy and Power Systems, King Abdulaziz University, Jeddah, Saudi Arabia. One of his previous projects (funded by the British Council, £186k involves the design of power electronic topologies and smart controllers for energy storage and electric vehicles in the home microgrids. He also received the QNRF-National Priority Research Program (NPRP13S-108-200028), entitled "Impact Assessment of EV Charging Stations and Regulation Policies for Upcoming Active Distribution Network of Qatar Utility Grid" (2021–2024), funded to the tune of ≈$600k. His proposal "Electric Vehicles pOint Location optimization via VEhicular communications (EVOLVE)" has been funded by Marie Skłodowska-Curie Actions Staff Exchange (2022–2026) to the tune of £620k. He is a PI on the "Optimal Scheduling of Electric Vehicle-Integrated Multi-Energy System With High Renewable Generation" funded by EPSRC through DTE Network+. He is also a PI on "Bi-Directional MIMO DC/DC Converter for V2G/X Infrastructures" (in collaboration with Otaski ES), funded by Innovative U.K. (≈£300k).

ALIASGHAR BAZIAR received the Ph.D. degree from Azad University, Iran, in 2022. He has seven years of working experience as a Senior Engineer in different parts of the industry and five years as a Faculty Member with Azad University. His research interests include power system operation and management, optimization in power systems, renewable energy sources, and uncertainty modeling.